Traveling-Wave Directional Filters with Transmission Zeros using Cross Coupling

Jakub Sorocki, Kamil Staszek, Ilona Piekarz, Slawomir Gruszczynski, and Krzysztof Wincza

***Abstract*— In this paper, a novel topology of a traveling-wave directional filter allowing for selectivity enhancement without increasing filter's order is proposed. Additional loose cross coupling introduced between #(n-1)th loop resonator and isolated port of the n^{th}-order directional filter allows for generating transmission zeros in the bandpass branch. Moreover, electrical length of the cross-coupling connecting transmission line allows for adjusting the location of transmission zeros and realizing symmetric or asymmetric frequency response. The presented approach is theoretically analyzed and experimentally verified. Exemplary second- and third-order directional filters with symmetrically placed transmission zeros were designed to operate at f_0 = 1 GHz, manufactured and measured. The obtained results prove correctness and applicability of the presented approach.**

***Index Terms*—cross coupling; directional filter; traveling-wave resonator; transmission zero.**

I. Introduction

DYNAMIC development of wireless systems enforces necessity of an appropriate management of available frequency spectrum, therefore, the development of novel frequency multiplexers and de-multiplexers featuring improved parameters has been a subject of extensive research over the last years. Among others, directional filters (DF) [1]-[12] were proven to be well suitable for application in de/multiplexers. The advantages of such circuits are modular construction and good impedance match over a wide frequency range. Thus, the entire system, that allows for frequency channel separation can be realized by cascading separately designed filters element by element, what is important when a large number of channels is required [12]. Generally, DFs can be divided into three categories according to their topology i.e., waveguide [2], standing wave [1], [8] and traveling-wave [2], [4]-[7], [9]-[11], for which various techniques allowing for realization of filters featuring appropriate bandpass and bandstop operation were investigated. In order to increase selectivity i.e., to increase the attenuation slope at band edges of such filters, one needs to increase the order of the filter, hence the number of wave-long loop resonators. On the other hand, selectivity can be increased while keeping the filters` order by introduction of transmission zeros into the bandpass path located closely outside the passband. Such an approach was presented e.g., in [10]-[11], where it was shown that the appropriate cascade connection of two identical directional filters allows to introduce transmission zeros. Alternatively, in [13] an asymmetric response fiber loop optical filter with additional cross-coupling was proposed for application in wavelength multiplexers. The desired frequency characteristics were achieved by coupling a small fraction of the power from one of the center loops to the isolated port.

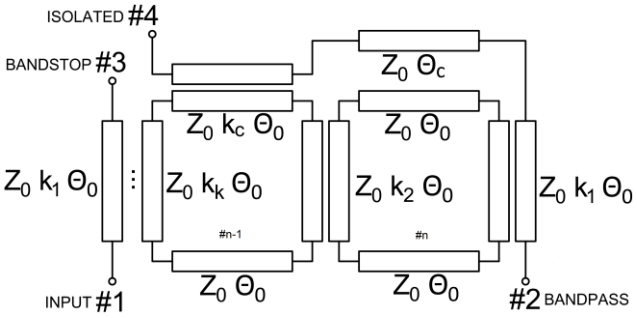

Fig. 1. General schematic diagram of the proposed n^{th}-order traveling-wave directional filter with additional cross coupling to provide two transmission zeros in the bandpass path. The order of the filter is increased by adding wave-long loop resonators coupled in between couplers k_1 and k_k. Please note, that the coupling coefficients are symmetrical with respect to symmetry axis. Z_0 is the system impedance, θ_0 = 90° @ f_0 while θ_c allows for tuning the location of transmission zeros.

In this paper, we propose a novel topology of an n^{th}-order (n > 1) traveling-wave directional filter allowing for the introduction of transmission zeros into the bandpass branch. The increased selectivity of the filter is obtained by means of additional loose cross coupling between #(n-1)th loop resonator and isolated port, thus the filters` order is unchanged. The proposed approach allows for reducing filters` area for a given selectivity as well as reducing total insertion losses in comparison to the filter with no transmission zeros, since the number of cascaded wave-long loop resonators is reduced. Such a feature may be especially useful for directional filters` application in high-power systems. The proposed approach is theoretically investigated in detail for a second- and third-order filter topologies. Moreover, a classic topology with no cross-coupling is considered for comparison purposes. The proposed design methodology is experimentally verified by the design of an exemplary second- and third-order

This work was supported by the National Science Centre in part under grant no. 2014/13/N/ST7/01961 and in part under grant no. 2016/23/D/ST7/00481. Moreover, Jakub Sorocki has obtained financial support under the PhD scholarship funded by the National Science Centre no. 2016/20/T/ST7/00202.

The authors are with the AGH University of Science and Technology, 30059 Krakow, Poland, phone: +48-12 617-34-93, e-mails: jakub.sorocki@agh.edu.pl, kstaszek@agh.edu.pl, ilona.piekarz@agh.edu.pl, slawomir.gruszczynski@agh.edu.pl, krzysztof.wincza@agh.edu.pl.

directional filters with symmetrically placed transmission zeros. Two filters operating at the center frequency of f_0 = 1 GHz have been manufactured and measured. The obtained results prove correctness and applicability of the proposed approach.

II. Introduction of Transmission Zeros Using Cross Coupling

General schematic of the proposed n^{th}-order traveling-wave directional filter with additional cross coupling is presented in Fig. 1. Such a filter is composed of at least two traveling-wave loop resonators and an additional path providing loose cross coupling k_c between #(n-1)th loop resonator and the isolated port #4. Each loop resonator is composed of two transmission-line sections having total electrical length of half-wavelength and two quadrature coupled-line directional couplers, what creates a wave-long loop. The band of interest is coupled from the input port #1 to the bandpass port #2 while creating bandstop at port #3. Order of the filter depends on the number of loop resonators and can be increased by adding loop resonators coupled in-between k_1 and k_k.

In general, behavior of the directional filter i.e., bandwidth of such filters as well as passband ripple in the bandpass path and stopband rejection in the bandstop path depend on coupling level between consecutive loop resonators, hence directional coupler's coupling level k_1 to k_k (note that coupling coefficients are symmetrical with respect to symmetry axis). Additionally, appropriate coupling level k_C allows for creating transmission zeros while electrical length θ_C allow for controlling their location. In order to design the n^{th}-order directional filter, one need to find a set of the above-mentioned coupling coefficients for a given bandwidth, bandstop attenuation/passband ripple and location of the transmission zeros.

A. Analysis of directional filters

Properties of the proposed directional filters` topology were assessed based on their *S*-parameters. A multielement multiport network analysis using connection scattering matrix approach [14], [15] was used, allowing for calculating directional filters` *S*-parameters based on *S*-parameters of the constitutive elements i.e., directional couplers and transmission lines. All ports within the multiport network are assumed to share a global ground node and identical characteristic impedance Z_0. For such a case, each node can be mapped to a port and the total number of nodes is equal to $N = N_1 + N_2$, where N_1 are the external ports of the circuits visible after matrix reduction while N_2 are the internal ports. The entire network is composed of M sub-networks, the *S*-parameters of which are known and the global wave equation can be obtained by proper indexing:

$$\begin{bmatrix} \boldsymbol{b} \\ \boldsymbol{b}` \end{bmatrix} = \begin{bmatrix} \boldsymbol{S}^A & \boldsymbol{S}^B \\ \boldsymbol{S}^C & \boldsymbol{S}^D \end{bmatrix} \begin{bmatrix} \boldsymbol{a} \\ \boldsymbol{a}` \end{bmatrix} \tag{1}$$

where

$$\boldsymbol{b} = \left[b_1 b_2 \dots b_{N_1}\right]^T, \boldsymbol{a} = \left[a_1 a_2 \dots a_{N_1}\right]^T \tag{2a}$$

$$\boldsymbol{b}` = \left[b_{N_1+1} b_{N_1+2} \dots b_N\right]^T, \boldsymbol{a}` = \left[a_{N_1+1} a_{N_1+2} \dots a_N\right]^T \tag{2b}$$

The connectivity at the internal ports can be expressed as:

$$\boldsymbol{b}` = \boldsymbol{\Lambda a}` \tag{3}$$

Eq. (1) and (3) can be simplified as follows:

$$\boldsymbol{b} = [\boldsymbol{S}^A + \boldsymbol{S}^B(\boldsymbol{\Lambda} - \boldsymbol{S}^D)^{-1}\boldsymbol{S}^C]\boldsymbol{a} \tag{4}$$

Therefore, the effective scattering matrix is equal to:

$$\boldsymbol{S}^{eff} = \boldsymbol{S}^A + \boldsymbol{S}^B(\boldsymbol{\Lambda} - \boldsymbol{S}^D)^{-1}\boldsymbol{S}^C \tag{5}$$

In this case, elements of the connectivity matrix can be determined using:

$$\Lambda_{ij} = \begin{cases} \frac{1}{P_i}(2 - P_i) & i = j \\ \frac{2}{P_i} & i \neq j \end{cases} \tag{6}$$

where $i, j = 1{:}N$ and P_i is the number of ports connected to the i-th node.

A numerical approach with optimization algorithm using nonlinear least-squares solver in *Matlab* software was employed to find relationship between coupling coefficients, electrical lengths, filters` bandwidth, filters` selectivity and location of transmission zeros. For all considered cases, the bandstop response S_{31} with in-band attenuation better than 20 dB is assumed together with an equal-ripple Chebyshev bandpass response S_{21}. Moreover, ideal match at each port is assumed. Directional filters` bandwidth is defined as:

$$BW_{3dB} = \frac{f_U}{f_L} \tag{7}$$

where f_U and f_L are upper and lower cut-off frequencies.

B. Second-order directional filter

The lowest order of the directional filter that can be realized using the proposed approach is n = 2 since the cross-coupling path is introduced between isolated port and #(n-1) loop resonator. Hence, the second-order directional filter, namely *DF2l2* is considered at first. A general schematic of such a filter is shown in Fig. 2a. Moreover, a classic second-order directional filter shown in Fig. 2b with no cross-coupling, namely *DF2no* is also analyzed for comparison purpose.

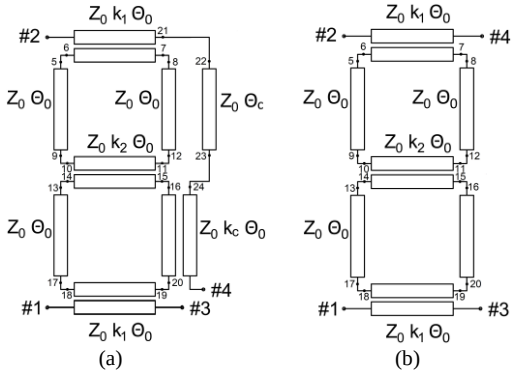

Fig. 2. General schematic of a 2nd-order traveling-wave directional filter with the proposed cross-coupling topology *DF2l2* (a) and a classic topology *DF2no* (b). For the analysis, Z_0 = 50 Ω and θ_0 = 90° are assumed.

Sets of coupling coefficients ensuring a given bandwidth were found as described in Section IIA for both filters and shown in Fig. 3. Moreover, equal ripple bandpass path characteristic and minimal stopband path attenuation of 20 dB were assumed within the band of interest. As seen, the proposed directional filter with additional cross coupling does not require higher maximal coupling level than the classic topology, which is especially of importance when wider filters` bandwidth is required.

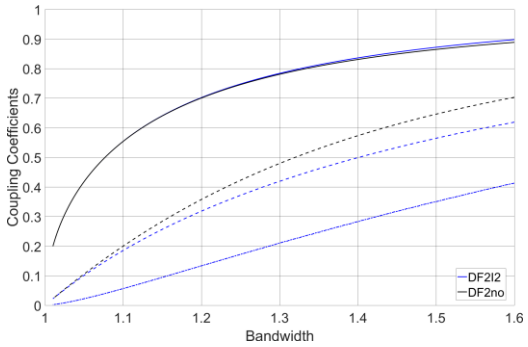

Fig. 3. Comparison of coupling coefficients k_1-k_2, k_C required to obtain a given bandwidth with stopband rejection better than 20 dB for 2nd-order directional filters with additional cross coupling path (DF2l2) and without one (DF2no).

Following, the selectivity of the bandpass path, defined as a ratio of bandwidths taken at 3 dB and 33 dB points of pass-band attenuation $SEL = BW_{3dB} / BW_{33dB}$, was calculated for both circuits, i.e., proposed and classic ones. The results are provided in Fig. 4. It can be clearly seen, that the proposed approach allows for a significant improvement, especially when wider filter` bandwidth is required.

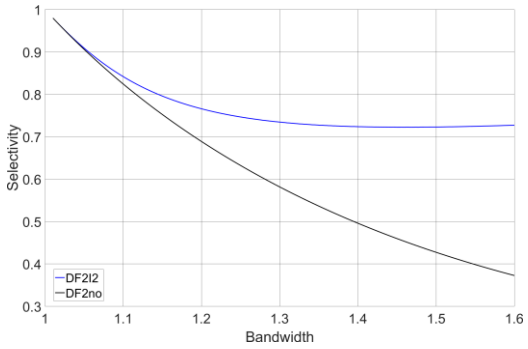

Fig. 4. Comparison of selectivity obtained for a given bandwidth for 2nd-order directional filters with additional cross coupling path (DF2l2) and without (DF2no). Selectivity of the passband path calculated as $BW_{3dB}/BW_{33\,dB}$.

Finally, a relationship between the location of the created transmission zeros f_{TZlow} and f_{TZhigh} vs. the electrical length θ_C was found and is provided in Fig. 5. As seen for $\theta_C = 90°$, the frequency response is symmetrical with respect to center frequency. Moreover, an asymmetric frequency response can be easily obtained with a very convenient control mechanism, independent from design parameters related to bandwidth and in-band ripple design.

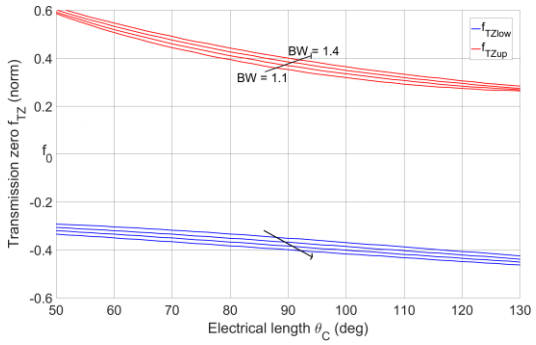

Fig. 5. Location of transmission zeroes with respect to the center frequency as a function of electrical length of the connecting transmission line θ_C calculated for various bandwidths.

C. Third-order directional filter

Following, the third-order directional filter, namely *DF3l2* is investigated. A general schematic of such a filter is shown in Fig. 6a. Moreover, a classical third-order directional filter, namely *DF3no*, shown in Fig. 6b is also analyzed for comparison purpose.

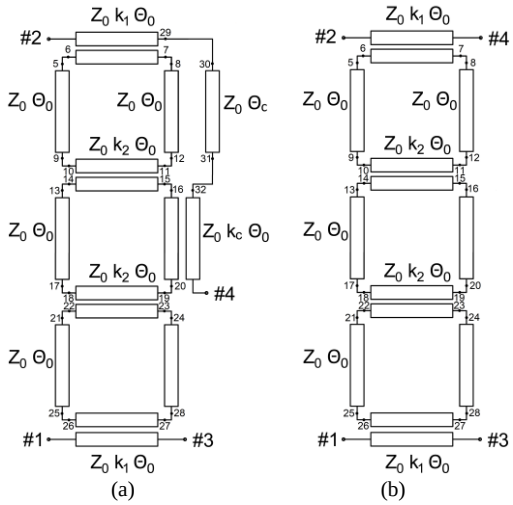

Fig. 6. General schematic of a 3rd-order traveling-wave directional filter with the proposed cross-coupling topology *DF3l2* (a) and a classic topology *DF3no* (b). For the analysis, $Z_0 = 50\ \Omega$ and $\theta_0 = 90°$ are assumed.

Similarly, as for the previous case, sets of coupling coefficients ensuring a given bandwidth were found for both filters and shown in Fig. 7. Also, identical requirements for bandpass and bandstop characteristics were assumed. As seen, the proposed topology requires slightly higher maximal coupling level than the classic topology when a wider bandwidth is required, still, the maximal coupling is within easily realizable range. Moreover, data for *DF3l2* is provided only for bandwidths within which the assumed frequency response constrains are met. Even though the range of realizable bandwidths is lower than in case of *DF2l2* for this particular set of goals, a superior out-of-band passband attenuation is obtained.

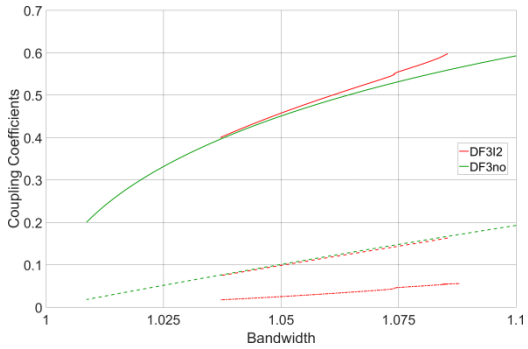

Fig. 7. Comparison of coupling coefficients k_1-k_2 & k_C required to obtain a given bandwidth with stopband rejection better than 20 dB for 3rd-order directional filters with additional cross coupling path (DF3l2) and without (DF3no).

Following, the selectivity of the bandpass path, defined as $SEL = BW_{3dB} / BW_{53dB}$, was calculated for both circuits i.e., proposed and classic one. Bandwidth at points of 53 dB attenuation on the attenuation slope was taken due to sharper filter`s slope. The results are provided in Fig. 8. It can be seen, that the selectivity of the *DF3l2* is increased with respect to the classic circuit, however, qualitatively the increase is smaller than for the second-order directional filter. It must be noted, however, that a third-order filter provides much higher out-of-band attenuation in the bandpass path. Hence for such a case greater improvement is seen when filter`s transition band (frequency range within cut-off frequency and frequency point of minimal out-of-band attenuation) is considered.

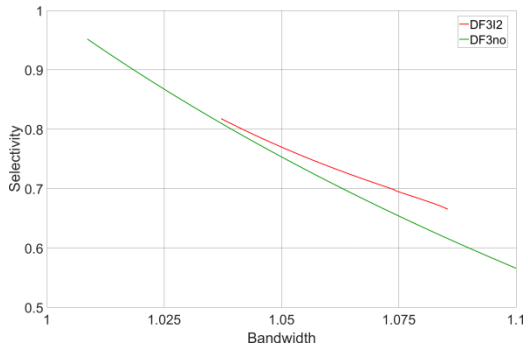

Fig. 8. Comparison of selectivity obtained for a given bandwidth for 3rd-order directional filters with additional cross coupling path (DF3l2) and without (DF3no). Selectivity of the passband path is calculated as BW_{3dB}/BW_{43dB}.

Finally, the relationship between the location of the created transmission zeros and the electrical length θ_C was found and is provided in Fig. 9. Similarly, as for the second-order filter, the location of transmission zeros can be conventionally designed with a symmetric frequency response being obtained for $\theta_C = 90°$.

The higher-order filters can be analyzed in the same fashion as the above presented cases using the approach described in Section II.A. Similar general behavior is expected, where introduction of loose cross-coupling generates additional transmission zeros located closely to center frequency and the increase of selectivity with respect to a classic topology.

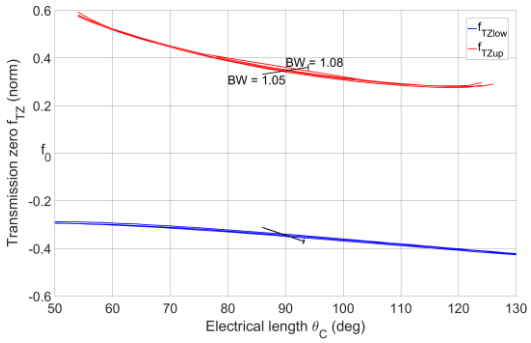

Fig. 9. Location of transmission zeros with respect to the center frequency as a function of electrical length of the connecting transmission line θ_C calculated for various bandwidths.

III. Experimental Results

The proposed directional filters` topology together with its theoretical analysis were experimentally verified by the design and measurements of two exemplary filters. A second and third-order traveling-wave directional filters with additional transmission zeros were realized to operate at the center frequency f_0 = 1 GHz with 120 MHz bandwidth (BW = 1.128) in 50 Ω system. Moreover, symmetric locations of transmission zeros with respect to the center frequency was assumed, hence $\theta_0 = \theta_C = 90°$. The methodology provided in Section II was used to determine the required coupling coefficients between each resonator. For the assumed bandwidth, the second-order filter requires the following couplings: k_1 = 0.619 (Z_{0e} = 103 Ω, Z_{0o} = 24.3 Ω), k_2 = 0.227 (Z_{0e} = 63 Ω, Z_{0o} = 39.6 Ω), k_C = 0.077 (Z_{0e} = 54 Ω, Z_{0o} = 46.3 Ω) to ensure minimal in-band bandstop path attenuation of 25 dB (see Fig. 10a). On the other hand, for the third-order filter the same set of couplings ensures minimal in-band attenuation of 14 dB (see Fig. 10b). For both filters, generated transmission zeros in the bandpass path are located ±360 MHz apart from the center frequency.

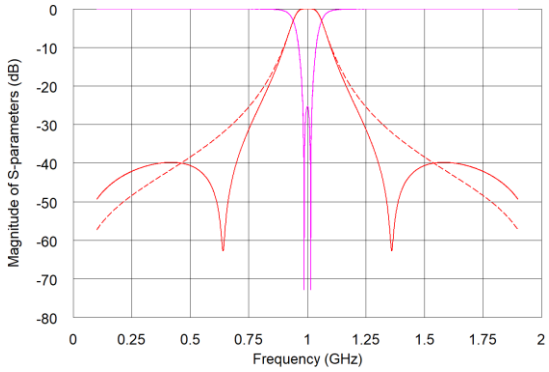

(a)

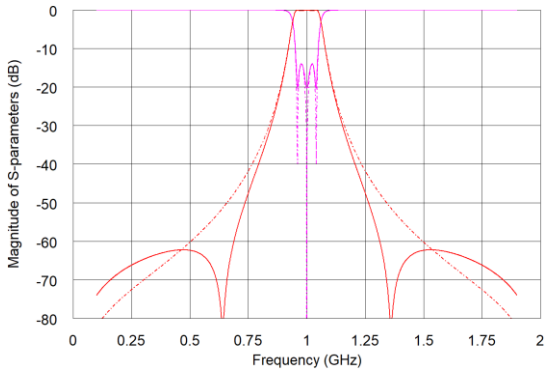

(b)

Fig. 10. Comparison of ideal-circuit *S*-parameters of the proposed directional filters with additional transmission zeros (solid line) and the classic ones (dashed lines). Identical bandwidths, in-band passband path ripples and in-band stopband attenuation are assumed. Second-order filter (a) and third-order filter (b); bandpass path (red) and bandstop path (pink).

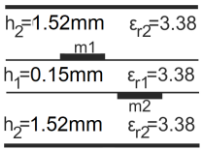

Fig. 11. Cross-sectional view of the stripline dielectric structure composed of three *Arlon 25N* laminates selected for the filters' design.

Stripline dielectric structure shown in Fig. 11 was used for the design, since it allows for a realization of relatively wide range of directional coupler`s coupling coefficients while ensuring that conditions of ideal coupled-line section realization are met [16]. *Linpar* [17] software was used to calculate initial geometry for each coupler i.e., strip widths` w_k and offsets o_k or spacing s_k, assuming that the couplers k_1 and k_2 are realized as a broadside coupled type while coupler k_C is realized as the edge-coupled-type coupler. Following dimensions were determined: w_{k1} = 0.95 mm, o_{k1} = 0.77 mm; w_{k2} = 1.69 mm, o_{k2} = 2.13 mm; w_{kC} = 1.84 mm, s_{kC} = 1.42 mm. Each directional filter was designed using *NI AWR Design Environment* software where each of the required couplers was analyzed and then connected using appropriate sections of transmission lines to create a set of coupled loop resonators. Transmission lines of the #n^{th} loop resonator were appropriately meandered to accommodate the physical length of the 90° cross-coupling path. Finally, the circuits were manufactured and measured. Picture of the assembly together with measured *S*-parameters of the second-order filter are shown in Fig. 12 and Fig. 13, respectively while for the third-order one in Fig. 14 and Fig. 15. The obtained performance for both circuits agrees with the designed one. The manufactured second-order filter operates at the center frequency of 1 GHz with 117 MHz bandwidth. Minimal in-band bandpass insertion losses equal 1.425 dB while the maximal in-band bandstop attenuation equals 20 dB. Return losses are better than 18 dB while isolation is better than 22 dB within the measured span. As predicted, additional transmission zeros are created in the bandpass path, located +390 MHz and -356 MHz apart from the center frequency.

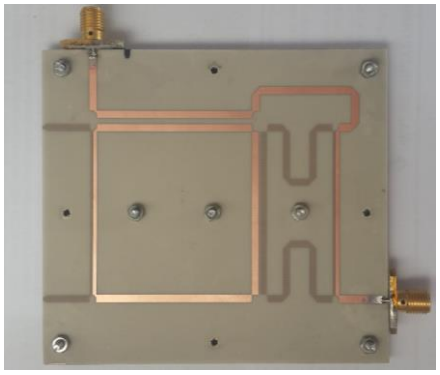

Fig. 12. Photograph of the inner thin laminate of the manufactured second order directional filter where cross coupling path can be clearly visible. The overall circuit's size equals 53.5 x 70.2 mm (excluding external transmission lines).

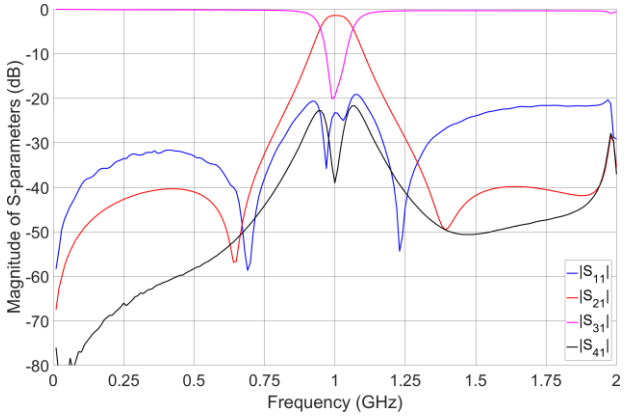

Fig. 13. Measured *S*-parameters of the manufactured 2nd-order directional filter with symmetrically placed transmission zeros.

The manufactured third-order filter operates at the center frequency of 1 GHz with 115 MHz bandwidth. Minimal in-band bandpass insertion losses equal 2.17 dB while in-band bandstop attenuation is within 14.4 dB and 26.4 dB. Return losses and isolation are better than 13 dB within the measured span. As predicted, additional transmission zeros are created in the bandpass path, located +368 MHz and -364 MHz apart from the center frequency.

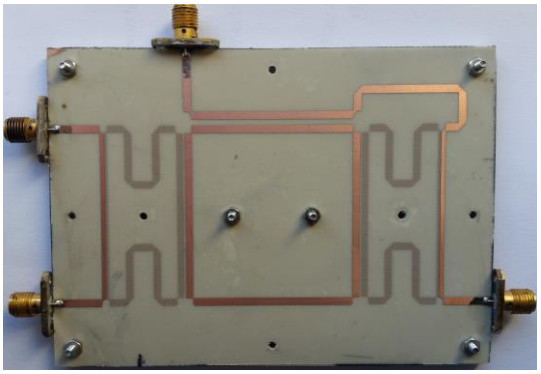

Fig. 14. Photograph of the inner thin laminate of the manufactured 3rd-order directional filter where cross coupling path can be clearly visible. The overall circuit size equals 53.5 x 88.5 mm (excluding external transmission lines).

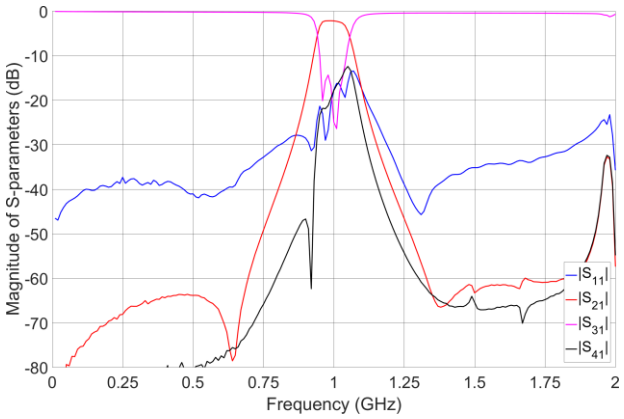

Fig. 15. Measured *S*-parameters of the manufactured 3rd-order directional filter with symmetrically placed transmission zeros.

The slight discrepancy between measured and calculated performance in both circuits is mostly a result of limited manufacturing and assembly tolerances. A very thin air layers are created in-between laminates what leads to a slight change in electrical lengths of transmission lines and slight change of coupling coefficient of couplers. This may affect the location of center frequency or location of transmission zeros and/or width of the passband.

IV. Conclusion

A novel topology of traveling wave directional filters allowing for selectivity enhancement without increasing filters order was proposed. It was shown that by introducing additional loose cross-coupling path between #(n-1)th loop resonator and isolated port of the nth-order filter, additional transmission zeros can be created in the bandpass path. Moreover, electrical length of the connecting transmission line allows for adjusting the location of transmission zeros. Because of the above-mentioned properties, such filters are well suitable for application in e.g., frequency multiplexers. A comprehensive theoretical study was provided for the proposed topology as well as for the classic one, allowing for investigating their behavior and presenting the advantages of the former ones. Moreover, experimental verification was provided by the design, manufacturing and measurement of exemplary second- and third-order directional filters featuring symmetrically placed transmission zeros. The obtained results agreed with the predicted filters` behavior confirming the correctness and usefulness of the proposed approach.

References

1. S. B. Cohn and F. S. Coale "Directional channel-separation filters," *Proc. IRE*, vol. 44, no. 8, pp. 1018-1024, 1956.
2. F. S. Coale "A traveling-wave directional filter," *IRE Transactions on Microwave Theory and Techniques*, vol. 4, no. 4, pp. 256-260, 1956.
3. F. S. Coale, "Applications of directional filters for multiplexing systems," *IRE Transactions on Microwave Theory and Techniques*, vol. 6, no. 4, pp. 450–453, Oct. 1958.
4. J. L. B. Walker, "Exact and approximate synthesis of TEM-mode transmission-type directional filters," *IEEE Transactions on Microwave Theory and Techniques*, vol. MTT-26, no. 3, pp. 186-192, Mar. 1978.
5. S. Uysal "Microstrip loop directional filter," *Electronics Letters*, vol. 33, no. 6, pp. 475-476, 1997.
6. S. Rosloniec and T. Habib, "Novel microstrip-line directional filters," *IEEE Transactions on Microwave Theory and Techniques*, vol. 45, no. 9 pp. 1633-1637, Sep. 1997.
7. Y. Cheng, W. Hong, and K. Wu, "Half-mode substrate integrated waveguide (HMSIW) directional filter," *IEEE Micowave and Wireless Components Letters*, vol. 17, no. 7, pp. 504-506, 2007.
8. J. S. Sun, H. Lobato-Morales, J. H. Choi, A. Corona-Chevez, and T. Itoh, "Multistage directional filter based on band-reject filter with isolation improvement using composite right-/left-handed transmission lines," *IEEE Transactions on Microwave Theory and Techniques*, vol. 60, no. 12, pp. 3950-3958, Dec. 2012
9. I. C. Hunter, E. Musonda, R. Parry, M. Guess, P. Sleigh, M. Gostling, and M. Meng, "Transversal directional filters for channel combining," *IET Radar, Sonar and Navigation*, vol. 8, no. 9, pp. 1288-1294, 2014.
10. J. Sorocki, I. Piekarz, S. Gruszczynski, and K. Wincza, „Cascaded loops directional filter with transmission zeroes for multiplexing applications," in Proc. *21st International Conference on Microwave, Radar and Wirelesss Communications (MIKON 2016)*, pp. 1-4, Krakow, Poland, 09-11 May, 2016
11. Y. Zhang, S. Shi, R. D. Martin and D. W. Prather, "Slot-coupled directional filters in multilayer LCP substrates at 95 GHz," *IEEE Transactions on Microwave Theory and Techniques*, vol. 65, no. 2, pp. 476-483, Feb. 2017
12. R. J. Cameron, and M. Yu, "Design of manifold-coupled multiplexers," *IEEE Microwave Magazine*, vol. 8, no. 5, pp. 46-59, Oct. 2007.
13. M. T. Wade, and M. A. Popovic, "Efficient wavelength multiplexers based on asymmetric response filters," *Optics Express*, vol. 21, no. 9, May 2013.
14. J. Dobrowolski, "Multielement multiport network analysis using connection scattering matrix approach," in *Microwave Network Design Using the Scattering Matrix*, 1st ed. Noorwood, MA: Artech House, 2010, ch. 5, sec. 5, pp. 120–124.
15. User`s Guide to S-parameters Explorer 2.0 EE Circle Solutions Dec. 2010, chapter 3.3.
16. K. Sachse, "The scattering parameters and directional coupler analysis of characteristically terminated asymmetric coupled transmission lines in an inhomogeneous medium," *IEEE Transactions on Microwave Theory and Techniques*, vol. 38, no. 4, pp. 417–425, Apr. 1990.
17. A. R. Djordievic, M. B. Bazdar, T. K. Sarkar and R. F. Harrington, *Matrix Parameters for Multiconductor Transmission Lines, Software and User's Manual*. Norwood, MA: Artech House, 1990.